

**SINGLE STATION EVENT LOCATION:
EPICENTRAL DISTANCE, BEARING, AND FOCAL DEPTH**

Jay Pulliam, Cliff Frohlich, and Ben Phillips
Institute for Geophysics, The University of Texas at Austin

Sponsored by the Defense Special Weapons Agency
Contract No. DSWA-01-97-0016

ABSTRACT

The most sensitive and reliable methods for locating small-magnitude regional seismic events using records from a single, three-component station require knowledge of the near-station and along-path crustal structure. Unfortunately, obtaining information about crustal structure is time-consuming and may be costly. Furthermore, different location methods may be required depending on the lateral complexity of the crust. Here we address a simpler problem: How often can single-station methods accurately determine event-station bearing and distance information if no information about crustal structure is available?

- Neither bearing nor distance determination was generally possible for signals if the SNR was less than about 2.0; bearing determination was most successful at most stations if signals were high-pass filtered with a cut-off frequency of about 0.5 Hz.
- Bearing determination for low-magnitude signals was possible even if they had no impulsive P phases if covariance methods were applied to the entire P-to-S time window.
- For signals with SNR > 2.0, there were clear differences between stations with respect to how well they could determine bearing direction. At many 'good' stations, 66% of the bearings determined by the 2-D covariance method were within about 6°-10° of the expected bearing; at many other stations, the 66th percentile of the bearings was 10°-30°.
- There were no obvious differences in the geographic or tectonic character of 'good' and 'other' stations.

Our original method for determining event-station distance relied solely on the ratios of short-term and long-term averages to find S-P times and thus distance; this method was able to determine distances to within 20 km of the true distance for only 10% of the records we studied. Currently, we are revising the phase-identification method to incorporate information about signal polarization.

Methods specifically designed for determining focal depths of events in sparsely-instrumented regions are rare. Here we apply a method for determining the focal depths of small- to moderate-sized earthquakes via waveform correlation between radial and vertical components of relatively high-frequency (1-5 Hz) seismic data recorded at a single three-component station and their synthetic counterparts. In addition to our waveform correlation method, which minimizes the complicating effects of the source time function and focal mechanism, we have begun to explore a strategy that exploits the expected simplicity of source time functions for small magnitude tectonic events and explosions. In this study we modify the deconvolution method of Christensen and Ruff (1984) and evaluate its applicability for focal depth determination at regional distances through a series of synthetic experiments.

OBJECTIVE

We are trying to develop, apply, and evaluate methods for locating seismic events using only a single, broadband, three-component seismographic station. Most of our work has been directed toward estimating the bearing and distance to and the focal depth of small-magnitude events located at regional distances from a station using full waveform data. A large percentage of seismic events could be identified as tectonic in origin if either or both the epicenter and/or focal depth were reasonably well-constrained. While approaches that use travel times and/or waveform data from several stations are well-developed, there are many regions of the world in which station coverage is sparse and small-magnitude events are often recorded by only one station, if at all.

RESEARCH ACCOMPLISHED

Single-Station Epicenter Location Without Special Knowledge of Crustal Structure

The bulk of our research effort has concerned developing location methods that rely on the comparison of observed and synthetic seismograms, and thus require knowledge of near-station crustal structure. However, to evaluate how much these methods improve location capabilities, we have also applied more simplistic methods to determine station event bearing and distance that require no knowledge of structure.

We therefore collected about 3800 three-component, digital waveforms for seismic events with reported magnitudes of 3.0-4.5 recorded at about 104 different stations distributed around the world. This search procedure produced records with highly variable amplitudes, including many low-SNR records in which the seismic signal was indistinguishable from the background. A preliminary analysis indicated that we could seldom obtain station-event bearings when the SNR for the time interval between P and S was less than about 2.0. Success rates for bearing determination were highest when the waveforms were high-pass filtered with a corner period T_F of about 2.0 sec. The restricted data set of records with SNR exceeding 2.0 included 1287 station-event pairs and included data from a broad variety of geographic and tectonic environments.

To determine station-event bearing, we used a 2-D method that separately determined the bearing axis (bearing angle mod 180°) and the bearing direction (see Magotra et al., 1987; Walck and Chael, 1991; Pulliam and Frohlich, 1998; 1999). We evaluated station-event bearing for the 1287 records for which SNR exceeded 2.0, applying the method to a 20-40-second interval beginning with the P arrival and ending prior to the arrival of S. To determine the event-station distance, we compared short-term and long-term signal averages to determine the time-separation between the onset times T_1 and T_2 of the two highest-amplitude portions of the waveform, and assigned a distance assuming that (T_2-T_1) corresponded to the S-P time interval.

These methods, which incorporate no information about regional crustal structure, were only partially successful at determining station-event bearing and distance. For the 1287 events, we obtained bearings within $\pm 10^\circ$ of the correct value for 54%, and within $\pm 20^\circ$ for 72%. For distance, the method was unable to determine any S-P interval for 41% of the signals; for the remaining 760 signals, the station-event distance was within ± 20 km for 18%, and within ± 50 km for 44%.

These low success rate suggest that it will be important develop location methods that incorporate information about regional crustal structure. Because the results indicate signals within P-to-S time interval generally are polarized along the event-station direction, we believe we can significantly improve station-event distance determination rates by developing a distance algorithm that incorporates both polarization and signal-to-noise information. However, even with these improvements it seems likely that a significant fraction of events will be mislocated unless more sophisticated algorithms that incorporate information about regional structure are developed.

Single-station Focal Depth Determination

We have presented results previously regarding the determination of event focal depths via waveform correlation to synthetic seismograms (Frohlich and Pulliam, 1999; Pulliam and Frohlich, 1998, 1999, 2000; Pulliam et al., 1997). We have recently focused on a new method for focal depth determination that makes use of the expected simplicity and short duration of source time functions for small-magnitude regional events. Christensen and Ruff (1984) presented a method for determining focal depths of large-magnitude, teleseismic events by deconvolving simple synthetic Green functions from the data to isolate the source time function. They show that when the incorrect depth is used for the Green functions, a complicated, oscillatory source time function of relatively long duration results. Using the correct focal depth for the Green functions produces a simpler and more realistic source time function of shorter duration. We seek to extend this method to small-magnitude, shallow seismic events recorded at regional distances and address several complicating issues through simulation with synthetic Green functions and various crustal structures. These issues include: the tradeoff between the source time function and focal depth, the required accuracy of the crustal model, the effects of the (presumably unknown) focal mechanism on the deconvolution and focal depth results, and the measure of source time function "simplicity" that points most reliably to the correct focal depth.

Tradeoff Between Source Time Function and Focal Depth

To explore the tradeoff between the source time function and estimates of focal depth we computed Green functions for a layer over a half-space model for a suite of focal depths from 0-15 km in increments of 2.5 km using a reflectivity method (Fig. 1). To illustrate the method we first construct synthetic radial and vertical component data by convolving Green functions for a 45 degree dip-slip fault with a source time function (Fig. 2). The source depth is 5 km. When each of the Green functions shown in Figure 1 is deconvolved from the synthetic data shown in Figure 2, the correct source time function is retrieved only for the correct focal depth of 5 km (Figure 3). Note that a similar function (with opposite polarity) also appears at the 5 km focal depth for the vertical strike-slip fault. In contrast, other source depths show a time lag for the source pulse plus a great deal of noise. This result indicates the tradeoff between origin time and the form of the source time function vs. focal depth. Since the estimate of origin time depends on crustal velocities as well as focal depth, the keys to reducing the ambiguity between the origin time and focal depth lie in the form of the source time function and the relative amplitudes of the source function and later parts of the seismogram. To construct a criterion for choosing the proper source time function we must make some assumptions about the source. For many sources of interest to CTBT discrimination—small-magnitude tectonic events and explosions—we expect the source time function to be relatively compact, short in duration, and “simple”, i.e., impulsive and unimodal, compared to large-magnitude shallow events that have large rupture surfaces. This suggests a criterion that favors compactness and high relative amplitudes early in the record compared to later parts of the record. After evaluating a number of candidates, we determined that a ratio of the norm of the deconvolved record’s first 10 seconds divided by the norm of the following 10 seconds was the most effective criterion. The maximum of this ratio of norms should indicate the correct focal depth. Figure 4 plots this ratio of norms as a function of focal depth for each of the fundamental faults, as computed for each of the deconvolved records shown in Figure 3. Radial and vertical components are computed separately, so their results are to some extent independent and a highly peaked function that is consistent result between the two components suggests minimal tradeoff and high confidence in the focal depth estimate. Note that, since each seismogram is produced by a single fault that resembles just one of the fundamental faults most closely, one should not expect a peak for each of the fundamental faults. Note, for example, that in Figure 3 the vertical dip-slip fault produces poor results after deconvolution. This poor result is reflected in the ratio of norms for the vertical dip-slip fault in Figure 4 (solid line).

Effect of Focal Mechanism on Deconvolution Results

An event’s focal mechanism changes the amplitude and polarity of each phase, which can complicate the deconvolution procedure. While it may be possible to find focal mechanisms for small-magnitude events with a single station, thereby allowing accurate modeling of seismograms, it may not be practical to do so, or to depend on the ability to do so. Regardless, it is instructive to examine the sensitivity of focal depth results to variations in the focal mechanism. Figure 5 shows one focal mechanism, in which the fault has a strike of 0° , dip of 10° , slip of 155° . The azimuth to the station is indicated by the thick solid line for each component. When the data shown in Figure 5 are deconvolved from the Green functions shown in Figure 1, the results (Figure 6) are more complex and less definitive than when the focal mechanism matches one of the fundamental faults (as in Figure 3). The noise in each record is of considerably higher amplitude (relative to the source pulse) and the source pulse distortion is more pronounced for all but the correct source depth. However, the “source simplicity” criterion is able to identify the correct focal depth, albeit with a norm ratio that is an order of magnitude smaller than the norm ratio in Figure 4. Figures 8-11 show focal depth results for deconvolutions of various focal mechanisms. All of these examples have “signal norm to noise norm” ratios between 1 and 8, compared to 20 for the first (ideal) case and all these depth functions are less peaked, indicating lesser depth resolution. However, only the vertical component of the last case (Figure 11) shows a real ambiguity in choosing the correct depth. Obviously, focal mechanisms in which critical phases exactly on nodal lines will not produce reliable results.

Effect of Inaccurate Crustal Velocity Model

To test the dependence of focal depth determinations on accurate knowledge of the crustal model, we conducted an experiment intended to mimic a potential procedure for finding focal depths with real data when we have limited information about the crustal structure in the vicinity of a seismographic station. We constructed a fairly complicated velocity model consisting of eight crustal layers on top of PREM (Fig. 12) and computed synthetic teleseismic data for a variety of focal mechanisms, focal depths, and epicentral distances (30° - 70°). We applied the SORVEC crustal receiver function method (Zhao and Frohlich, 1996; Zhao et al., 1996) to these data while specifying search limits that allowed models of various complexity: from three to seven layers with wide search

bounds for individual layers' thicknesses and shear and compressional wave velocities. This step produced a set of models (Fig. 12) that have similar bulk characteristics (average velocities and crustal thicknesses) but which differ in number of layers and the seismic velocities of each layer. These approximations are intended to represent estimates of crustal structure obtained using real data, which tend to match the real Earth in some characteristics (e.g., average crustal velocity, depth to Moho, etc.) but which fail to match finer details. The question we wish to answer is "How significantly can the model used to compute Green functions differ from the actual Earth and still produce accurate focal depth estimates via the "source simplicity" criterion?"

To address this question we compute suites of "reference" Green functions for each model, comparable to Figure 1, for an epicentral distance of 200 km and deconvolve each from "data" seismograms constructed using the original, eight-layer velocity model, the source time function shown in Figure 2, and various focal mechanisms. The resulting focal depth estimates are shown in Figures 13-17. Note the progressive loss of resolution as the model becomes less and less detailed and deviates more and more from the true, eight-layer model. If more depth increments had been used to compute Green functions, the depth functions in Figures 4, 7-11, and 13-17 would be smoother curves, with a less obvious peak. The choice of focal depth would therefore be less obvious and one's confidence in each focal depth estimate would diminish with successively less refined (and less accurate) models. This exercise demonstrates a tradeoff between the accuracy of the crustal model used to generate Green functions and depth resolution of event foci. Note also the drop in the ratio of norms between the seven-layer model (Figure 13) and the six-layer model (Figure 14), and continued decreases with each successive figure.

CONCLUSIONS AND RECOMMENDATIONS

The deconvolution method that relies on a "source simplicity" criterion presented here shows promise for discrimination between explosions and tectonic events. Christensen and Ruff (1984) make a strong case for the deconvolution method's effectiveness when applied to large-magnitude, deeper events recorded at teleseismic distances. Additional complications arise in extending the method to small-magnitude, shallow events recorded at regional distances. These include: poor signal-to-noise ratios, relatively high amplitudes of scattered waves that complicate the seismograms, a tradeoff between depth resolution and accuracy of the crustal model. Specifically, the following conclusions may be gleaned from our synthetic experiments:

- Successful application depends strongly on the accuracy of a crustal model's bulk characteristics but depends only weakly on details of the model, such as the number of layers and velocities of each layer.
- In contrast, knowledge of an event's focal mechanism is not critical; the simultaneous deconvolution of Green functions for the three fundamental fault types leads to accurate focal depth results.
- There is a fundamental tradeoff between depth resolution of event foci and accuracy of the crustal models used to compute Green functions. However, models that match the bulk characteristics of the real Earth may serve to identify the correct focal depth. But in all cases, confidence in the focal depth estimate will be enhanced by greater accuracy of the crustal model.

Lastly, we observe that the "source simplicity" method, like the waveform correlation method, depends on full waveform information, as opposed to travel times. It is the pulse distortion of the improperly deconvolved data that allows some reconciliation (however imperfect) of the focal depth vs. origin time/source time function tradeoff. Given the need to understand certain aspects of crustal velocity structure well, attention should be focused on developing practical methods for modeling crustal velocities.

Key Words: Single-station location, focal depth determination, regional seismology

REFERENCES

- Christensen, D. H., and L. J. Ruff (1984). Analysis of the trade-off between hypocentral depth and source time function, *Bull. Seismol. Soc. Am.*, **75**, 1637-1656.
- Frohlich, C., and J. Pulliam (1999). Single-station location of seismic events: A review, and a plea for more research, *Phys. Earth Planet. Int.*, **113**, 277-291.
- Magotra, N., N. Ahmed and E. Chael (1987). Seismic event detection and source location using single-station (three-component) data, *Bull. Seismol. Soc. Am.*, **77**, 958-971.
- Pulliam, J., and C. Frohlich (2000). Determining Earthquake Focal Depths with a Single Seismographic Station at Regional Distances, submitted to *Bull. Seis. Soc Am.*, May 2000.
- Pulliam, J., and C. Frohlich (1999). Accuracy and uncertainty in single-station event location, in *Proc. 21st Ann. Seismic Res. Symp.*, vol. I, tech. rept. No. LA-UR-99-4700, Dept. Defense, Arlington, Va., pp. 589-598.
- Pulliam, J., and C. Frohlich, Case Studies of Event Location with a Single Station, *Proceedings of the 20th Annual Seismic Research Symposium on Monitoring a Comprehensive Test Ban Treaty*, J. Fantroy, D. Heatley, J. Warren, F. Chavez, and C. Meade (edit.), Santa Fe, N.M., 275-285, 1998.
- Pulliam, J., C. Frohlich and S.P. Grand (1997). Factors controlling single-station seismic event location, *Proceedings of the 19th Annual Seismic Research Symposium on Monitoring a Comprehensive Test Ban Treaty*, M.J. Shore, R.S. Jih, A. Dainty, and J. Erwin (edit.), Orlando, FL, pp. 272-280.
- Walck, M. C. and E. P. Chael (1991). Optimal backazimuth estimation for three-component recordings of regional seismic events, *Bull. Seismol. Soc. Am.*, **81**, 643-666.
- Zhao, L.-S., and C. Frohlich (1996). Teleseismic body waveforms and receiver structures beneath seismic stations, *Geophys. J. Int.*, **124**, 525-540.
- Zhao, L.-S., Sen, M. K., Stoffa, P. L., and C. Frohlich (1996). Application of very fast simulated annealing to the determination of the crustal structure beneath Tibet, *Geophys. J. Int.*, **125**, 355-370.

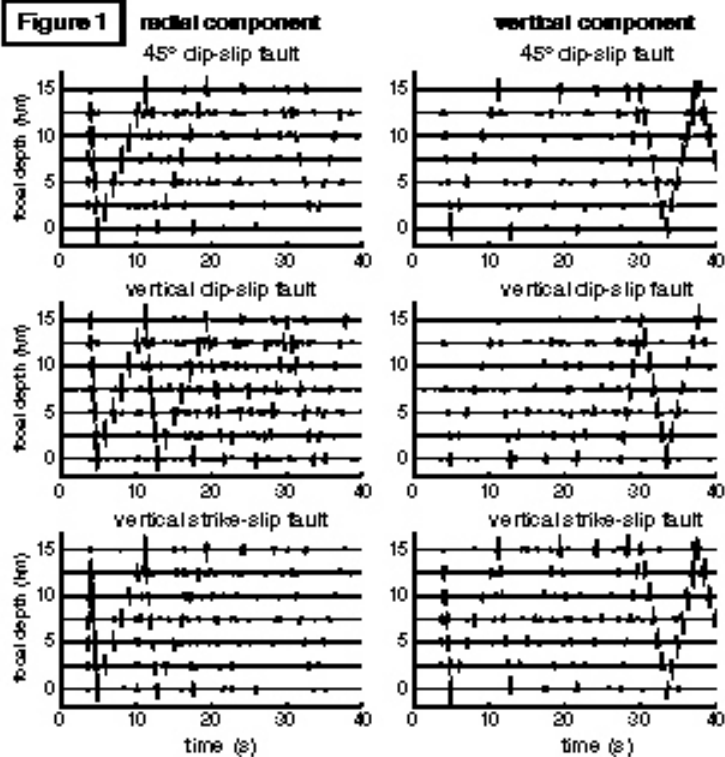
Figure 1

Figure 1. Radial and vertical component Green functions for three fundamental faults and focal depths of 0 to 15 km in increments of 2.5 km. These were computed using a reflectivity method and a simple layer over a half-space velocity model. The epicentral distance is 100 km.

Figure 2. Synthetic seismograms are constructed by convolving a source time function with the Green functions from Figure 1 for a 45° dip-slip fault and a focal depth of 5 km.

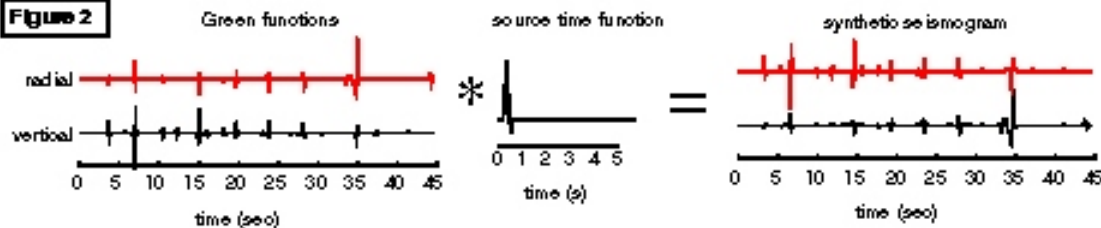
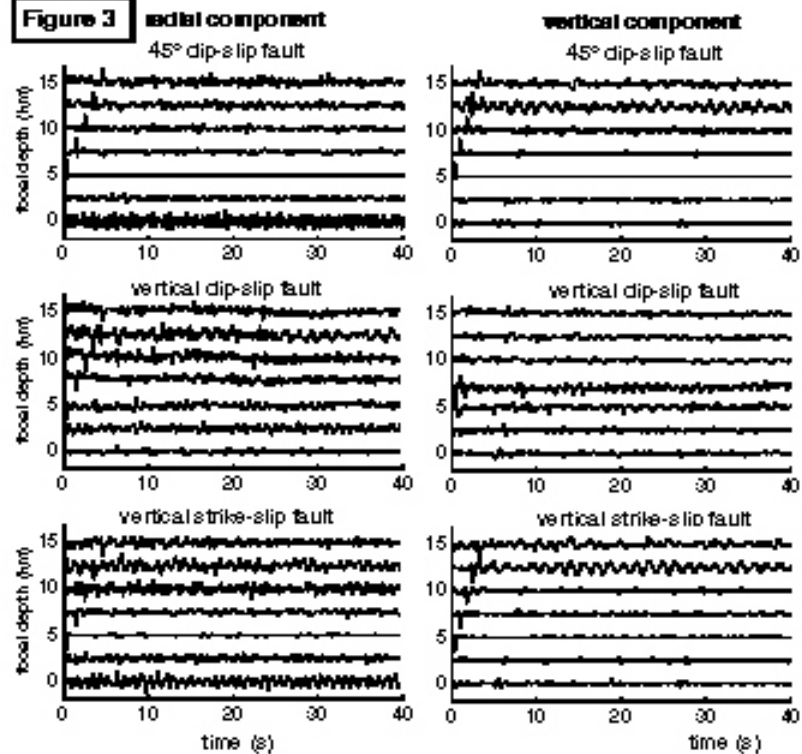
Figure 2**Figure 3**

Figure 3. The Green functions shown in Figure 1 are each deconvolved from the synthetic data shown in Figure 2. The result for the correct focal depth and fault type is simply the input source time function shown in Figure 2 (45° dip-slip fault and focal depth of 5 km) but results for other focal depths and fault types are more complex. The familiar tradeoff between origin time (onset of source time function) and focal depth is indicated by the increasing time lag for increasing focal depth but the more useful properties are the distortion of the pulses retrieved by the deconvolution and the relative amplitudes of the source pulse and the following noise.

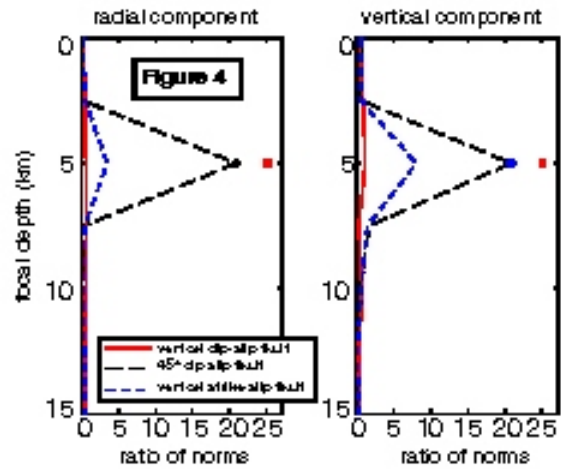


Figure 4. The correct pulse (by construction, in this case) is compact, short in duration, and has a large amplitude ratio when compared to later parts of the record. A criterion that favors these characteristics can be devised that is essentially the ratio between the norms of the record's first 10 seconds and the following 10 seconds. When plotted as a function of focal depth for each fault type, this ratio achieves a maximum at the correct focal depth. Obviously, inaccurate estimates of crustal structure and various focal mechanisms will degrade the strongly peaked ratio of norms and will thereby degrade depth resolution. The square at right indicates the correct focal depth.

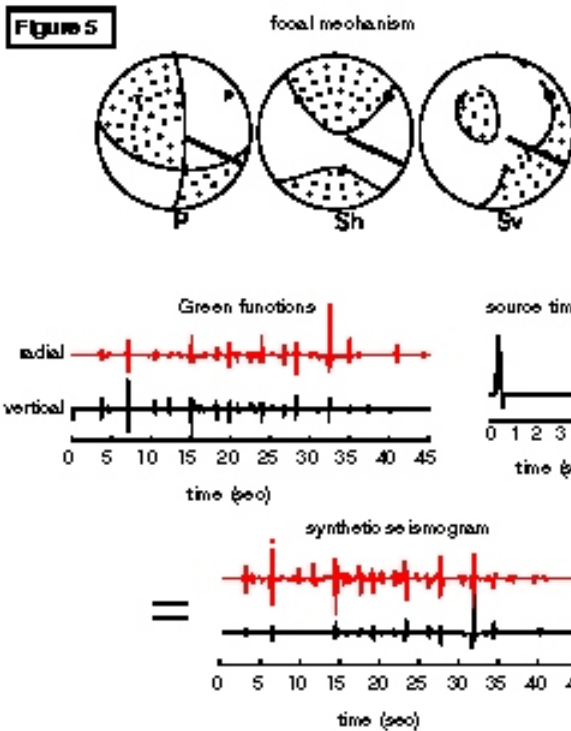


Figure 5. An example of the potentially complicating effect of a focal mechanism that differs from those of the fundamental faults. Synthetic data are again constructed but this time they incorporate the focal mechanism shown.

Figure 6. When the Green functions shown in Figure 1 are deconvolved from the data shown in Figure 5, a more complicated set of traces results. Noise is large in amplitude and the pulse distortion is more pronounced for all but the correct focal depth.

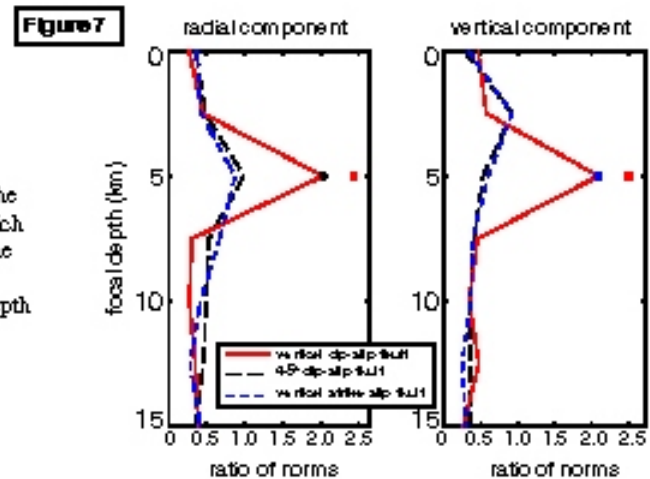
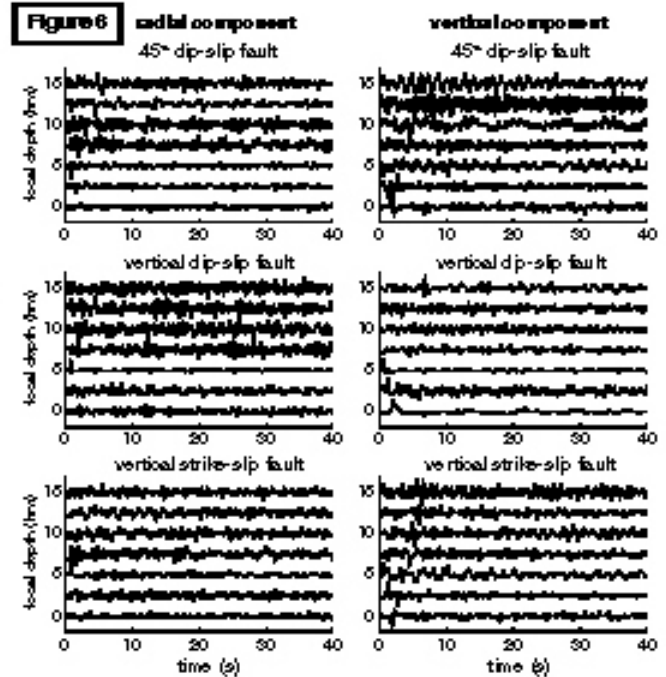
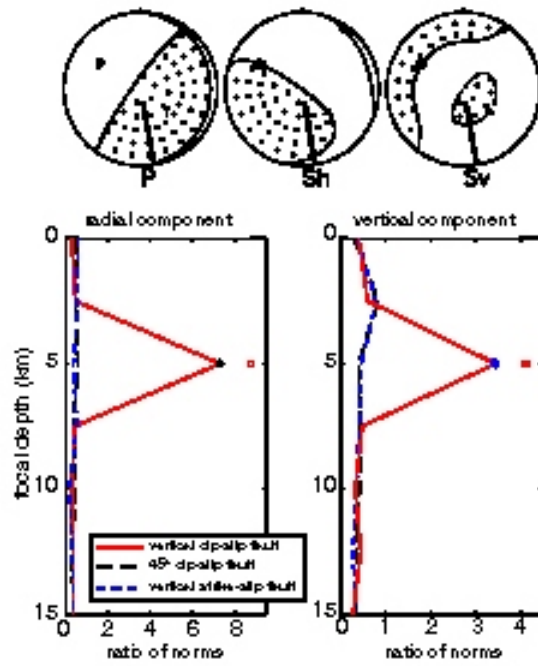
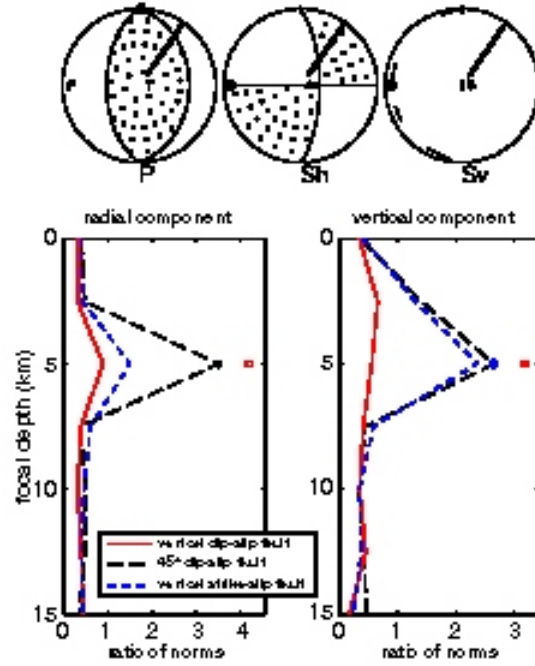
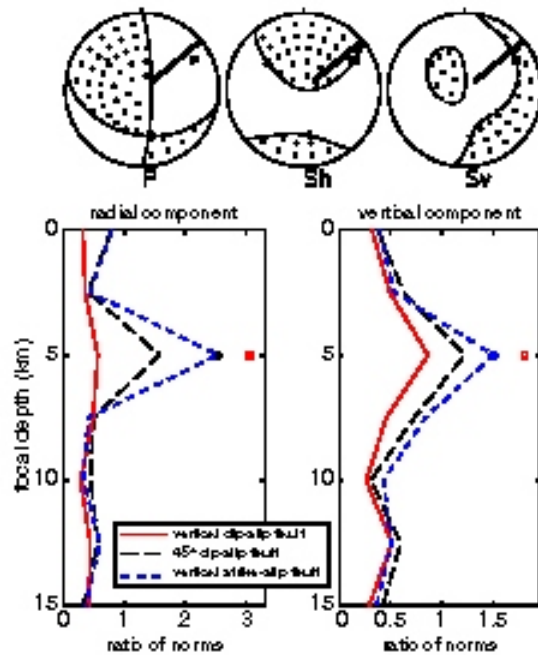
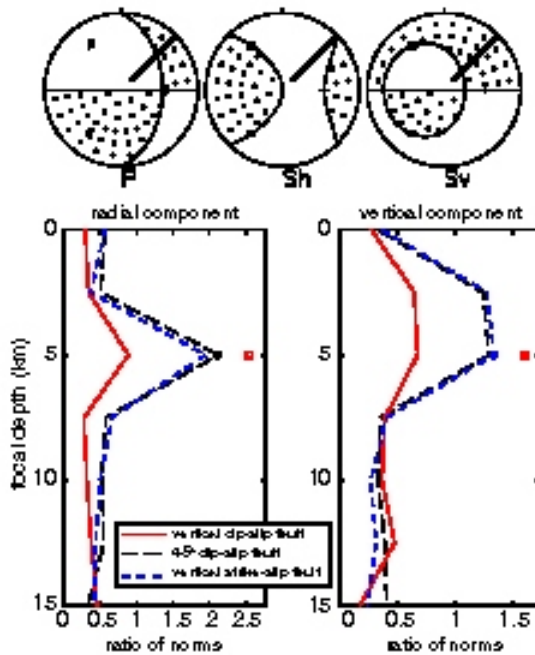


Figure 7. Note the much lower values for the ratio of norms compared to Figure 4, in which the focal mechanism of the data matched one of the fundamental faults. Nevertheless, a distinct peak identifies the correct focal depth and the focal depth resolution (spread or "peakedness" of the norm function through depth) is comparable.

Figure 8**Figure 9****Figure 10****Figure 11**

Figures 8-11. Various focal mechanism and their effects on the focal depth criterion. Note that in some cases the depth resolution is degraded (e.g., Figure 11), in which case the choice of focal depth is ambiguous. See the text for further discussion of depth resolution and confidence.

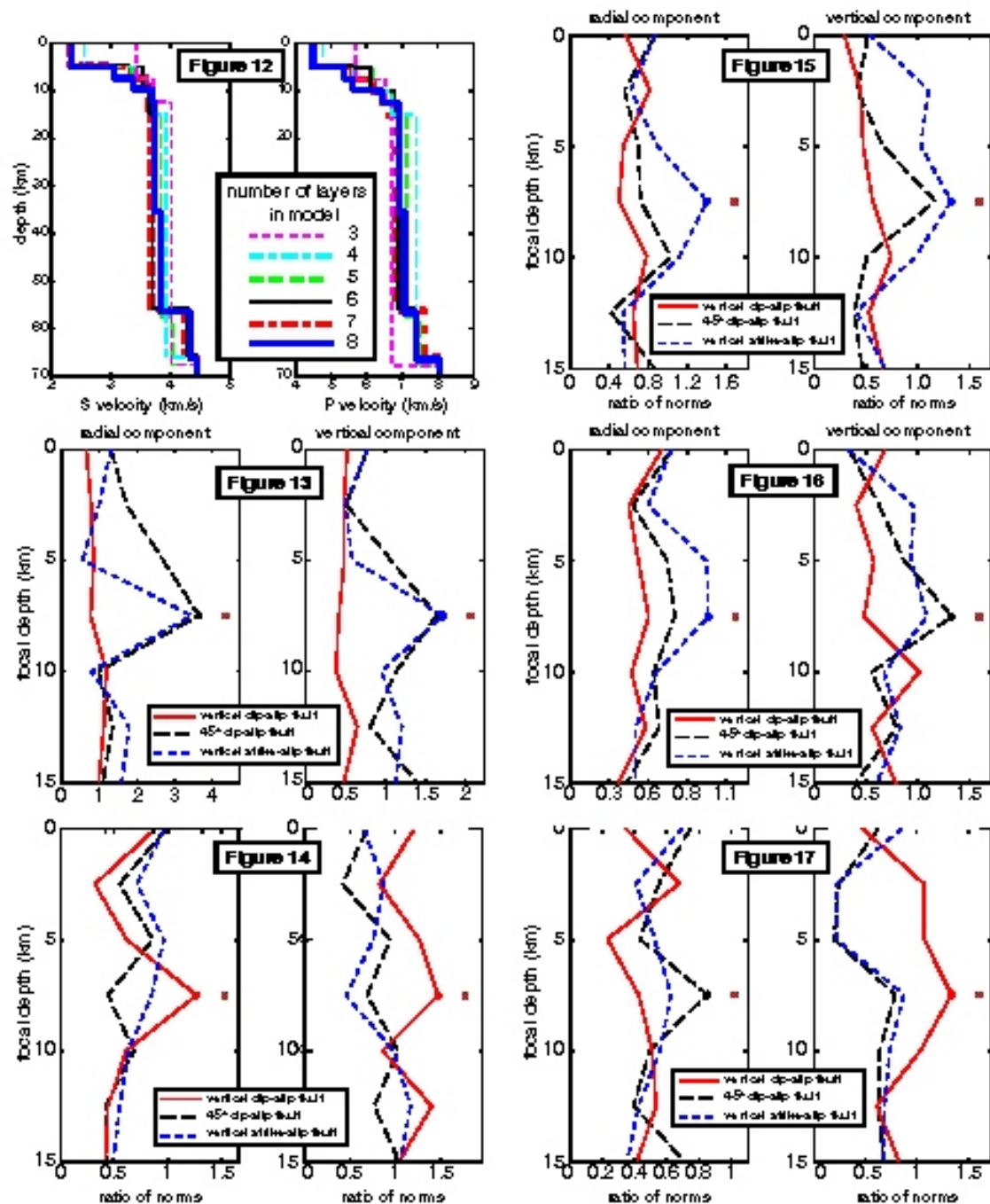


Figure 12. Velocity models obtained by applying the SORVEC method (Zhao and Frohlich, 1996) to synthetic synthetic seismograms computed for tele seismic distances (30° - 70°) using an eight-layer crustal model over PREM. Wide search bounds were prescribed for layer thicknesses and for compressional and shear wave velocities but the number of layers allowed was successively limited to seven, six, five, four, and three.

Figures 13-17. Results of deconvolving data constructed using the Green functions of $h=7.5$ km depth computed using the eight-layer velocity model (Fig. 12), the source time function shown in Figure 2 and various focal mechanisms from the models shown in Figure 12 that approximate the eight-layer input model in bulk characteristics but which lack similar levels of detail. Results for the "source simplicity" criterion are shown for models with seven layers (Fig. 13), six layers (Fig. 14), five layers (Fig. 15), four layers (Fig. 16), and three layers (Fig. 17). These approximations are intended to represent estimates of crustal structure obtained using real data, which tend to match the real Earth in some characteristics (e.g. average crustal velocity, depth to Moho, etc.) but which fail to match finer details. This series illustrates a tradeoff between depth resolution of event foci and accuracy of the reference crustal model.